

Supplementary Material A. Similarity Matrix Sparsification

As mentioned in Section 2.1, the use of the Gaussian similarity measure

$$w_{ij} = \exp\left(-r_{ij}^2/2\sigma^2\right) \quad (\text{A1})$$

in the similarity matrix \mathbf{W} greatly reduces the impact of the sparsification step compared to the l_x/r_{ij} measure used in Hadjighasem *et al.* [15]. This result is due to w_{ij} in (A1) approaching zero faster for large r_{ij} .

It is mentioned in Section 3.1, however, that sparsifying the matrix is worthwhile to reduce computational costs and storage, and we therefore sparsify entries of \mathbf{W} that satisfy $w_{ij} < \exp(-4^2/2)$, corresponding to $r_{ij} > 4\sigma$. This sparsification rule is used in Sections 3.2, 3.3, 3.4 and 4.1, under the assumption that such sparsification has negligible impact on the clustering membership probability results.

Here, we present a study for the Bickley jet system with model parameters as in Section 3 and method free-parameters $\sigma/l_x = 0.020$, $m = 2$, and $K = 7$, where the clustering is performed using different levels of sparsification. We vary the sparsification levels by setting $w_{ij} = 0$ for $r_{ij}/\sigma > \alpha$, with $\alpha \in \{0.5, 1, 2, 4, 8\}$ and $\alpha = \infty$ representing the non-sparsified result matching Figure 1(a).

Figure A1(a) presents a histogram with the distribution of r_{ij} values. The vast majority of these values represent the time-averaged distance between particles that describe dissimilar trajectories, and therefore correspond to graph edges of negligible weights. Figure A1(b) presents the weight dependence on r_{ij}/σ , and therefore the maximum magnitude of matrix entries that are dropped when \mathbf{W} is sparsified for a choice of α .

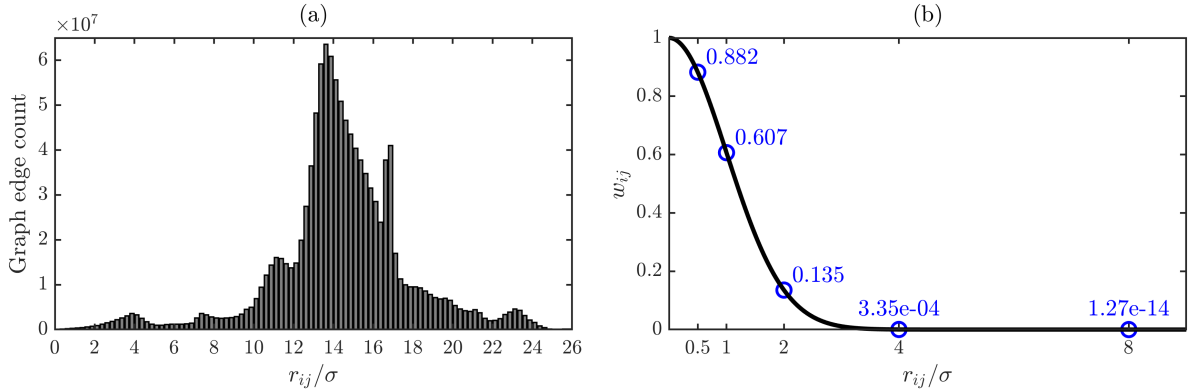


Figure A1. (a) Histogram of the time-averaged distance values, made dimensionless by $\sigma = 0.020/l_x$, with a bin width of 0.25. (b) Weight dependence on r_{ij}/σ for the Gaussian measure (A1). The w_{ij} values for $r_{ij}/\sigma = 0.5, 1, 2, 4$ and 8 are shown in blue.

The impact of the sparsification parameter α on the number of retained (nonzero) entries in the similarity matrix is shown in Table A1. For all finite choices of α presented here, the percent sparsification of \mathbf{W} is greater than 95%.

Table A1. Dependence of \mathbf{W} entries on the sparsification parameter α .

Sparsification parameter α	Number of nonzero entries in \mathbf{W}	Percent Sparsification (%)
0.5	287,852	99.99
1	1,078,658	99.95
2	5,052,598	99.78
4	38,712,302	98.32
8	99,413,096	95.69
∞	2,304,000,000	0

The cluster membership probabilities obtained with the different choices of α are presented in Figure A2. We notice that sparsifying with $\alpha = 0.5, 1$ or 2 clearly has an effect on the resulting membership probabilities, as clusters shrink as α is reduced. For $\alpha \geq 4$, however, the probabilities no longer depend on α , and no difference is observed between the method output for $\alpha = 4$ or the non-sparsified case ($\alpha = \infty$).

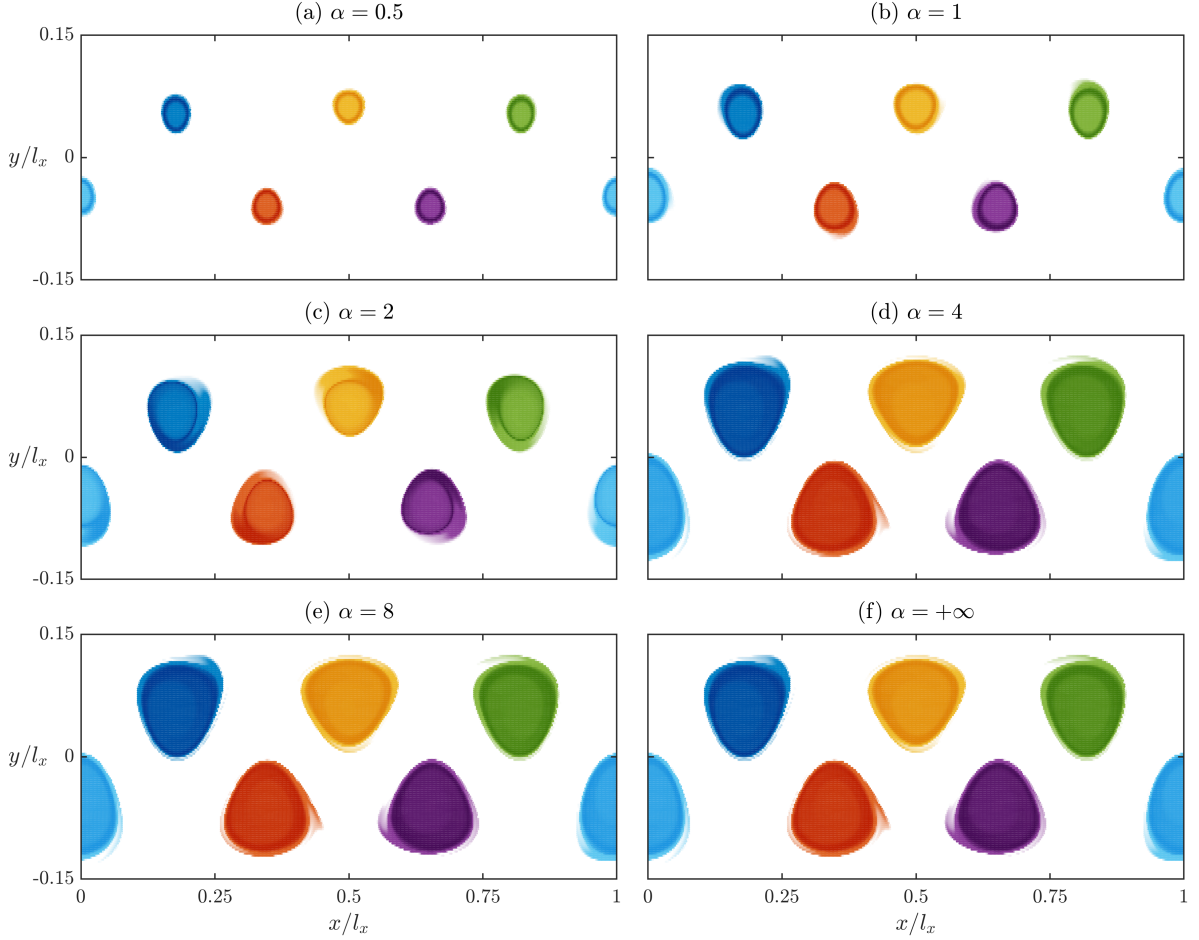


Figure A2. Membership probabilities for vortices $k \in \{1, \dots, 6\}$, for different choices of the sparsification parameter α , plotted at $t = t_0$. Values correspond to (a) $\alpha = 0.5$, (b) 1 , (c) 2 , (d) 4 , (e) 8 , and (f) $+\infty$. Corresponding colorbars presented in Figure 1

Sparsifying with $\alpha = 4$ also reduces the number of nonzero entries in \mathbf{W} by about 60 times, and therefore facilitates storage and reduces the computational time when solving the generalized eigenproblem. Note that this result is valid for the Bickley jet parameterized as in Section 3, but the impact of sparsification may vary for an arbitrary flow.